An Adaptive Signal Processing System for Active Control of Sound in Remote Locations

Iman Tabatabaei Ardekani* and Waleed H. Abdulla†
* Computing Dept., Unitec Institute of Technology, Auckland, New Zealand
† Electrical and Computer Eng. Dept., The University of Auckland, Auckland, New Zealand

***Abstract*—Adaptive active noise control (ANC) systems with single-channel structure create a silent point at the location of an error microphone. This silent point creates a zone of quiet surrounding itself, however, this zone has small dimensions. Moreover, the error microphone has to be located within the zone of quiet, limiting the effective space available in the zone of quiet. This paper develops a new adaptive signal processing system for ANC in a remote point, located far from the error microphone. Accordingly, the effective space of the zone of quiet can be extended. It is shown that an optimal controller for the creation of a remote silent point can be constructed by the series combination of a digital controller, called the remote controller, and an adaptive digital filter. The transfer function of the remote controller is derived based on the system model in the acoustic domain. A new update equation for the automatic adjustment of the adaptive digital filter is proposed. The validity of the results is discussed through different computer simulations.**

I. Introduction

Active noise control (ANC) has been paid attention in the control of low frequency sound fields, where the sound wavelength is greater than acoustic barriers dimensions [1]. Several approaches have been so far used for the development of ANC systems, resulting in different types of controllers for ANC, e.g. analog feedback controllers [2], internal model-based controllers [3] and adaptive digital filters (ADF) [4]–[6]. Among them, adaptive filters show a high level of reliability and efficiency in different ANC applications. The first attempts to apply adaptive signal processing techniques for developing ANC systems were reported by Burgess [4] and Warnaka [5], independently. Burgess proposed a single-channel feed-forward structure for adaptive ANC and derived the Filtered-x Least Mean Square (FxLMS) algorithm as the key component of this structure. Elliott proposed a multichannel structure for adaptive ANC and developed a multichannel FxLMS algorithm [7]. Eriksson introduced the feedback structure as an alternative to the feedforward structure [8]. The original FxLMS algorithm, derived by Burgess [4], is today known as a fundamental algorithm for adaptive ANC. Widrow derived a similar algorithm in the context of adaptive control for adaptive inverse control problems [9]. In the past few years, the authors have extensively studied the behaviors of the FxLMS algorithm in ANC applications [10]–[14], resulting in determining restrictions of available adaptive ANC systems, one of which is addressed in this paper.

The FxLMS algorithm adaptively adjusts a secondary sound field in accordance with the information provided by a reference microphone and an error microphone. The secondary

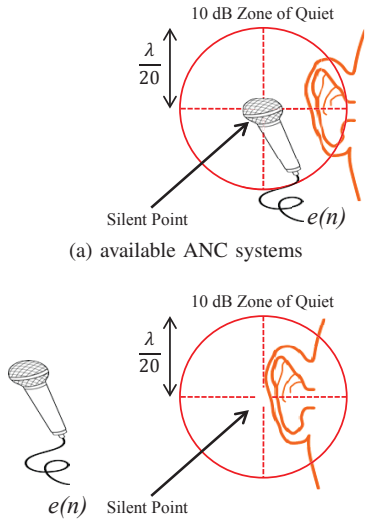

(a) available ANC systems

(b) proposed ANC system

Figure 1: locations of silent point, zone of quiet and error microphone

field, that is sometimes called the anti-noise field or control field, is superposed to the primary sound field (or noise field). The superposition of the two fields minimizes the sound field at the location of the error microphone. In this situation, a silent point is created at the error microphone location and, consequently, a zone of quiet is produced around this point as a byproduct. A single silent point in a pure-tone diffuse sound field establishes a spherical zone of quiet with at least 10 dB noise reduction within its volume (10 dB zone of quiet) [15]. As seen in Fig. 1a, the 10 dB zone of quiet is centered at the silent point and its radius is $\frac{\lambda}{20}$, where λ is the wavelength. Technically, single-channel ANC systems are only able to make small zones of quiet. For example, in a 750 Hz pure-tone sound field ($\lambda \approx 45.7$ cm), the radius of the zone of quiet is limited to 2.2 cm. Additionally, the error microphone has to be located at the center of the quiet zone, resulting in a very small space for even a human ear to be located in the zone of quiet. For solving this problem, a multichannel structure for adaptive ANC can be used. In this case, several error microphones and several control loudspeakers are used to create several silent points [16]. Consequently, the available silent points can make a larger zone of quiet. This improvement can be achieved only at the cost of using several microphones, loudspeakers and using more hardware resources for implementing a multichan-

nel FxLMS algorithm. One solution is to apply virtual sensing mechanisms [17]. Based on this approach, new applications of adaptive ANC systems can be investigated [18], [19]. In [20], an adaptive signal processing system was proposed based on virtual sensing to remove the error microphone from the zone of quiet. This system was originally proposed for the ANC-based hearing aids, where locating an error microphone within the zone of quiet (eardrum) is technically impossible. As an additional advantage, the effective space within the zone of quiet is extended because there is no error microphone in the zone. The main drawback of this system is its computational complexity due to inverting and computing several matrices.

The main motivation of this study is to develop a new adaptive signal processing system for creating a silent point and, consequently, a zone of quiet at a remote location, far from the error microphone. In this case, the effective space of the zone of quiet can be extended. The desired locations of the error microphone, silent point and zone of quiet are shown in Fig. 1b. Compared to the ANC system introduced in [20] and [21], the proposed system is more computationally efficient because it does not require inverting and computing matrices. Compared to multichannel ANC systems, the proposed system is more economically efficient. This is because this system does not require additional hardware components rather than those required by a typical single-channel feedforward ANC system.

The rest of the paper is organized as follows. Section II describes a typical FxLMS-based adaptive ANC system and analyzes its behavior in both the acoustic and digital electronic domains. Section III describes the idea of remote ANC and develops a new adaptive signal processing algorithm for performing active control of sound in remote locations. Section IV discusses computer simulation results. Finally, Section V gives concluding remarks.

II. Modeling FxLMS-based ANC

Fig. 2 shows a typical layout and block diagram for FxLMS-based adaptive ANC [1]. In this figure, G and H represent two physical sub-systems of the ANC plant, called the primary and secondary paths respectively. They are unknown systems that model the sound propagation in the ANC plant. The reference signal, $x\left(n\right)$, is measured by a microphone located close to the noise source. The error signal, $e\left(n\right)$, is measured by the error microphone, located at the desired silent point. The digital controller, W is a finite impulse response (FIR) filter that generates the control signal, $y\left(n\right)$, to drive the control source. The sound produced by the control source has to pass H to reach the error microphone. On the other hand, the original noise, produced by the noise source, has to pass G to reach this point. These two signals combine acoustically with each other across the acoustic domain. However, $e\left(n\right)$ that is the net sound pressure at the location of the error microphone is only taken as the measure of the residual noise. Consequently, an adaptive ANC system can adjust W only in such a way that the measured signal $e\left(n\right)$ to be minimized. In the following the behaviors of the typical ANC model shown in Fig. 2 are analyzed in both the acoustic and digital electronic domains.

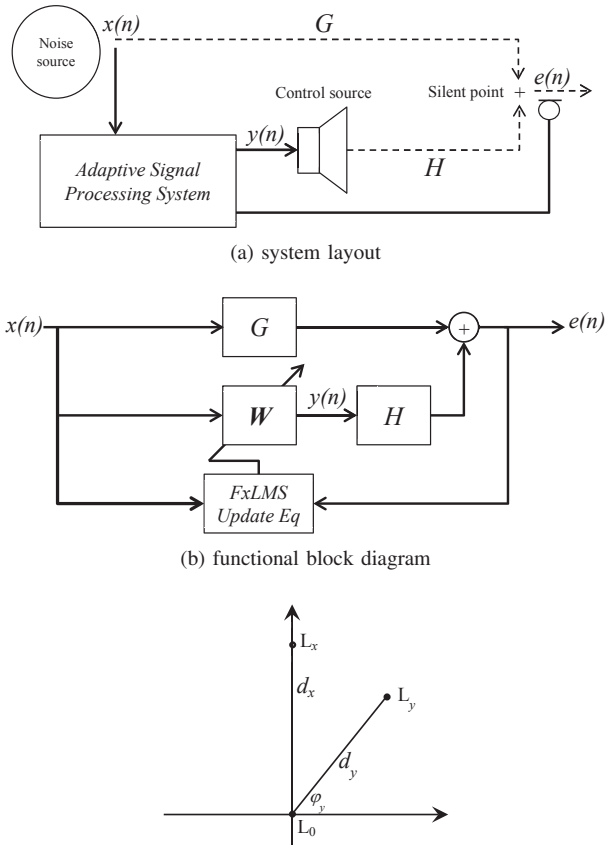

(a) system layout

(b) functional block diagram

(c) locations of noise source (L_x), control source (L_y) and error microphone (L_0)

Figure 2: modeling a typical ANC system (single-channel feed-forward structure)

A. Acoustic Domain

In order to study ANC system behaviors in the acoustic domain, it is first required to determine the locations of the system components in a coordinate system. In a general case, the noise source, the control source and the error microphone are located in three arbitrary points L_x, L_y and L_0, respectively. Assuming that L_x, L_y and L_0 are non-collinear, a unique plane always passes through them. The x-y plane of the coordinate system is set to this plane. The y-axis is set to the line passing through L_0 and L_x. The origin of the coordinate system is set to L_0. This unique coordinate system along with the location of the ANC system components are shown in Fig. 2c. As shown in this figure, the control source location can be specified by a radial distance, d_y, and a polar angle, φ_y. Also, the noise source location is specified by a radial distance, d_x, and a polar angle, $\frac{\pi}{2}$.

Now let us assume that the noise source is a monopole source, generating a stochastic sound in the acoustic domain. The reference microphone is located close to the noise source; therefore, the noise field at the location of the error microphone (L_0) is

$$p_0\left(n\right) = \frac{1}{d_x} x\left(n - \tfrac{d_x}{c}\right) \tag{1}$$

where $x\left(n\right)$ is the reference signal and c is the sound velocity.

Similarly, assuming that the control source is a monopole source that generates the control signal $y(n)$ in the acoustic domain, the anti-noise field at L_0 is

$$q_0(n) = \frac{1}{d_y} y\left(n - \tfrac{d_y}{c}\right) \tag{2}$$

The net sound pressure at L_0 is the superposition of $p_0(n)$ and $q_0(n)$:

$$e(n) = p_0(n) + q_0(n) \tag{3}$$

A silent point at L_0 can be created when a control signal $y(n)$ causes $e(n)$ to be zero. This control signal, denoted by $y_{opt}(n)$, is obtained by setting Eq. (3) to zero after substituting Eqs. (1) and (2) into it:

$$y_{opt}(n) = -\frac{d_y}{d_x} x\left(n - \tfrac{d_x - d_y}{c}\right) \tag{4}$$

Eq. (4) can be expressed in the z-domain by

$$Y(z) = K_{xy} z^{-\Delta_{xy}} X(z) \tag{5}$$

where $X(z)$ is the z-transform of $z(n)$, Δ_{xy} is a time-delay and K_{xy} is a static gain given by

$$\Delta_{xy} = \frac{d_x - d_y}{c} \tag{6}$$

and

$$K_{xy} = -\frac{d_y}{d_x} \tag{7}$$

From Eq. (5), the transfer function of the optimal controller can be obtained:

$$W_{opt}(z) = \frac{Y(z)}{X(z)} = K_{xy} z^{-\Delta_{xy}} \tag{8}$$

In the derivation of Eq. (8), the uncertainties associated with the sound propagation, e.g. sound reflection and reverberation, are not considered. For solving this problem, we propose to re-express Eqs. (1) and (2) as follows:

$$p_0(n) = \frac{1}{d_x} u_x(n) \circledast x\left(n - \tfrac{d_x}{c}\right) \tag{9}$$

$$q_0(n) = \frac{1}{d_y} u_y(n) \circledast y\left(n - \tfrac{d_y}{c}\right) \tag{10}$$

where $\circledast$ is the linear convolution operator and where $u_x(n)$ and $u_y(n)$ are two unknown transfer functions modeling possible reflections, reverberations and any other uncertainties associated with the sound propagation. Now by substituting Eqs. (9) and (10) into Eq. (3) and by following the same steps taken for the derivation of Eq. (8), a more realistic solution for $W_{opt}(z)$ can be obtained:

$$W_{opt}(z) = \frac{U_x(z)}{U_y(z)} K_{xy} z^{-\Delta_{xy}} \tag{11}$$

where $U_x(z)$ and $U_y(z)$ are the z-transforms of $u_x(n)$ and $u_y(n)$. The direct implementation of the optimal transfer function given in Eq. (11), or even the one given in Eq. (8), is not technically possible because it requires geometrical parameters and acoustical characteristics of the physical plant, i.e. $U_x(z)$ and $U_y(z)$, to be known.

B. Digital Electronic Domain

From the block diagram given in Fig. 2b, one can find that for $e(n) = 0$, the controller should be set to $W_{opt} = GH^{-1}$. This solution corresponds to the solution given in Eq. (11). The main problem here is that G and H are unknown systems. For solving this problem, the FxLMS algorithm (or FxLMS update equation) is used to adjust W adaptively, until it converges to W_{opt}. Concurrently, the error signal power converges to a minimal level. The FxLMS update equation is given by

$$\mathbf{w}(n+1) = \mathbf{w}(n) + \mu e(n) \mathbf{x}_H(n) \tag{12}$$

where μ is the adaptation step size and the weight vector $\mathbf{w}$ (of length L) is formed by the impulse response coefficients of W:

$$\mathbf{w}(n) = \begin{bmatrix} w_0(n) & w_1(n) & \dots & w_{L-1}(n) \end{bmatrix}^T \tag{13}$$

$\mathbf{x}_H(n)$ is the filtered-x vector, calculated by filtering a tap vector of the reference signal, $\mathbf{x}(n)$, with an estimate of the secondary path H. Assuming that an accurate estimate of H is available, $\mathbf{x}_H(n)$ can be formulated by

$$\mathbf{x}_H(n) = \sum_{q=0}^{Q-1} h_q \mathbf{x}(n-q) \tag{14}$$

where h_0, h_1, ..., h_{Q-1} are the impulse response coefficients of H and the tap vector $\mathbf{x}(n)$ is given by

$$\mathbf{x}(n) = \begin{bmatrix} x(n) & x(n-1) & \dots & x(n-L+1) \end{bmatrix}^T \tag{15}$$

Now that an updated weight vector for W is computed by Eq. (12), the control signal $y(n)$ can be computed as the response of W to the reference signal:

$$y(n) = \mathbf{w}(n)^T \mathbf{x}(n) \tag{16}$$

A loudspeaker can be then used to transfer $y(n)$ to the acoustic domain. The function of this signal in the acoustic domain is discussed in the previous subsection. The FxLMS algorithm is designed in such a way that W converges to the optimal controller that minimizes the power of $e(n)$. This optimal solution corresponds to the transfer function given in Eq. (11).

III. Remote Active Noise Control

In this paper, it is desired to create a silent point at a remote location on the x-axis, L_r, while the error microphone located at the origin is untouched. Figs. 3 show the general layout of the desired system. Fig. 4 shows the locations of the system components in the defined coordinate system. In this figure, the distance between L_r and the feedback microphone (origin) is modeled by d.

A. Acoustic Domain Analysis

The net sound field at L_r is given by

$$e_r(n) = p_r(n) + q_r(n) \tag{17}$$

where $p_r(n)$ and $q_r(n)$ are the sound fields generated by the noise source and control source at L_r respectively. Using the

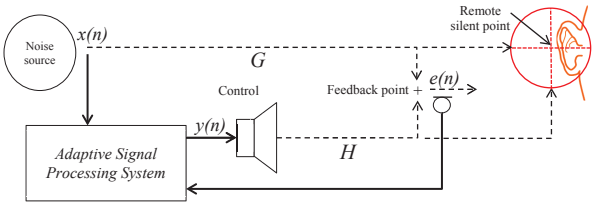

Figure 3: remote ANC layout (proposed system)

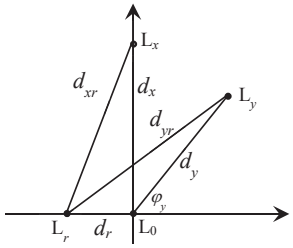

Figure 4: locations of noise source (L_x), control source (L_y), error microphone (L_0) and remote silent point (L_r)

same logic used for the derivation of Eqs. (9) and (10), $p_r(n)$ and $q_r(n)$ can be obtained as

$$p_r(n) = \frac{1}{d_{xr}} u_x(n) \circledast x\left(n - \tfrac{d_{xr}}{c}\right) \tag{18}$$

$$q_r(n) = \frac{1}{d_{yr}} u_y(n) \circledast y\left(n - \tfrac{d_{yr}}{c}\right) \tag{19}$$

It is assumed that $u_x(n)$ and $u_y(n)$ do not change because d_r is very shorter than the distances of L_x and L_y from the origin. A silent point at the remote location L_r can be created when for a control signal $y(n)$, $e_r(n)$ becomes zero. This control signal, denoted by $\tilde{y}_{opt}(n)$, can be obtained by setting Eq. (17) to zero after substituting Eqs. (18) and (19) into it:

$$\tilde{y}_{opt}(n) = -\frac{d_{yr}}{d_{xr}} u_x(n) \circledast u_y^{-1}(n) \circledast x\left(n - \tfrac{d_{xr}-d_{yr}}{c}\right) \tag{20}$$

Therefore, the optimal transfer function for creating a silent point at the remote location L_r is:

$$\tilde{W}_{opt}(z) = \frac{Y(z)}{X(z)} = \frac{U_x(z)}{U_y(z)} \tilde{K}_{xy} z^{-\tilde{\Delta}_{xy}} \tag{21}$$

where time-delay $\tilde{\Delta}_{xy}$ and static gain $\tilde{K}_{xy}$ are given by

$$\tilde{\Delta}_{xy} = \frac{d_{xr} - d_{yr}}{c} \tag{22}$$

$$\tilde{K}_{xy} = -\frac{d_{yr}}{d_{xr}} \tag{23}$$

The direct implementation of $\tilde{W}_{opt}(z)$ is not technically possible because acoustical characteristics and geometrical parameters of the physical plant are unknown (because $U_x(z)$ and $U_y(z)$ are unknown transfer functions). Alternatively, an adaptive algorithm can be used to identify an estimate of $\tilde{W}_{opt}(z)$. In this application (remote ANC), the FxLMS algorithm cannot be used because it requires the error microphone to be placed at the desired silent point (that is the remote point L_r here). In the following, a new adaptive algorithm to be used for remote ANC is developed.

B. Adaptive Identification of Optimal Controller

From Fig. 4, the distance between L_x and L_r is

$$d_{xr} = \sqrt{d_x^2 + d_r^2} \tag{24}$$

For $\frac{d_r}{d_x} \ll 1$, Eq. (24) can be approximated by the first two terms of its Taylor series:

$$d_{xr} \approx d_x \left(1 + \tfrac{d_r}{d_x}\right) \tag{25}$$

Similarly, the distance between L_y and L_r is

$$d_{yr} = \sqrt{d_y^2 + d_r^2 + 2 d_r d_y \cos\varphi_y} \tag{26}$$

For $\frac{d_r}{d_y} \ll 1$, Eq. (26) can be approximated by the first two terms of its Taylor series

$$d_{yr} \approx d_y \left(1 + \tfrac{d_r}{d_y} \cos\varphi_y\right) \tag{27}$$

Substituting Eqs. (24) and (27) into Eq. (22) results in

$$\tilde{\Delta}_{xy} = \frac{d_x - d_y + d_r - d_r \cos\varphi_y}{c} \tag{28}$$

By using Eq. (6), $\tilde{\Delta}_{xy}$ can be re-expressed by

$$\tilde{\Delta}_{xy} = \Delta_{xy} - \frac{d_r}{c}(1 - \cos\varphi_y) \tag{29}$$

Also, substituting Eqs. (24) and (27) into Eq. (23) results in

$$\tilde{K}_{xy} = -\frac{d_y \left(1 + \tfrac{d_r}{d_y} \cos\varphi_y\right)}{d_x \left(1 + \tfrac{d_r}{d_x}\right)} \tag{30}$$

For $\frac{d_r}{d_x} \ll 1$,

$$\frac{1}{1 + \tfrac{d_r}{d_x}} \approx 1 - \tfrac{d_r}{d_x} \tag{31}$$

Substituting Eq. (30) into (31) results in

$$\tilde{K}_{xy} = -\frac{d_y}{d_x}\left(1 - \tfrac{d_r}{d_x} + \tfrac{d_r}{d_y}\cos\varphi_y - \tfrac{d_r^2}{d_x d_y}\cos\varphi_y\right) \tag{32}$$

which can be approximated by

$$\tilde{K}_{xy} = -\frac{d_y}{d_x}\left(1 - \tfrac{d_r}{d_x} + \tfrac{d_r}{d_y}\cos\varphi_y\right) \tag{33}$$

By using Eq. (7), $\tilde{K}_{xy}$ can be re-expressed by

$$\tilde{K}_{xy} = K_{xy}\left(1 - \tfrac{d_r}{d_x} + \tfrac{d_r}{d_y}\cos\varphi_y\right) \tag{34}$$

Now, combining Eqs. (21), (29) and (34) results in

$$\tilde{W}_{opt}(z) = \frac{U_x(z)}{U_y(z)} K_{xy} K_\rho z^{-(\Delta_{xy} + \Delta_\rho)} \tag{35}$$

where time-delay Δ_ρ and static gain K_ρ are given by

$$K_\rho = 1 - \frac{d_r}{d_x} + \frac{d_r}{d_y}\cos\varphi_y \tag{36}$$

and

$$\Delta_\rho = \frac{d_r}{c}(1 - \cos\varphi_y) \tag{37}$$

From Eqs. (11) and (35), $\tilde{W}_{opt}(z)$ can be expressed by

$$\tilde{W}_{opt}(z) = \rho(z) W_{opt}(z) \tag{38}$$

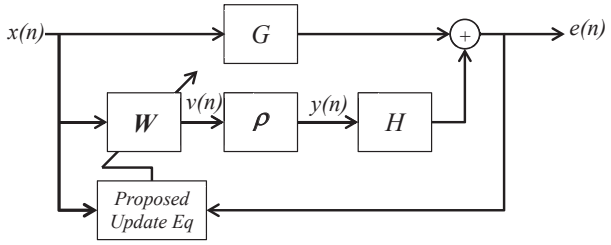

Figure 5: functional block diagram of remote ANC (proposed system)

where $\rho(z)$ is the remote controller transfer function, given by

$$\rho(z) = K_\rho z^{-\Delta_\rho} \tag{39}$$

Eq. (38) gives the transfer function of the optimal controller $\tilde{W}_{opt}(z)$ that creates a silent point at a remote location. According to Eq. (38), the proposed ANC controller is obtained by the series combination of a remote controller, $\rho(z)$, and a traditional ANC controller, $W_{opt}(z)$. Based on this finding, the functional block diagram of the remote ANC system can be developed as shown in Fig. 5. Note that $W_{opt}(z)$ is the transfer function of an optimal controller that could have minimized the sound field at the location of the error microphone (origin of the coordinate system). In the proposed system, $W_{opt}(z)$ is a part of the remote ANC system; therefore, it does not intend to minimize the sound field at the error microphone location. Alternatively, it intends to contribute in the minimization of the sound field at a remote location far from the error microphone.

1) Construction of the remote controller $\rho(z)$: Eqs. (36), (37) and (38) give a transfer function for the construction of the remote controller. This controller is always stable and causal because it has a pure-delay impulse response with a positive semi-definite time-delay. Based on these equations, the construction of the remote controller requires the location of the noise source (d_x), the location of the control source (d_y and φ_y) and the distance of the remote silent point from the error microphone (d_r) to be known.

2) Construction of the traditional ANC controller $W_{opt}(z)$: In the traditional ANC, an estimate of $W_{opt}(z)$ is identified by the FxLMS algorithm, as discussed in Subsection II-B. In this case, unknown acoustical characteristics of the physical plant and the uncertainties associated with the system model are taken into account while $W_{opt}(z)$ is being identified adaptively. The FxLMS algorithm is able to arrive at an estimate of $W_{opt}(z)$, if the reference and error signals fed to its update equation are identical to those of the original FxLMS-based ANC system; but we have changed the control system structure by introducing the remote controller $\rho(z)$. The reference signal is independent of the control system; therefore, the reference signal of the remote ANC system (shown in Fig. 3) is identical to that of the original FxLMS-based ANC system (shown in Fig. 2a). Unlike the reference signal, the error signal is affected by the remote controller $\rho(z)$. Therefore, the error signal in the remote ANC system is different with the error signal in the original FxLMS-based ANC system.

For solving this problem, we can compensate for the influences of the remote controller $\rho(z)$ on the error signal, resulting in a new adaptive ANC algorithm to be used in remote ANC applications. From the block diagram given in Fig. 2b, the error signal in the original FxLMS-based ANC system can be expressed in the z-domain:

$$E^*(z) = G(z)X(z) + W(z)H(z)X(z) \tag{40}$$

Similarly, the error signal in the remote ANC system can be expressed from the block diagram shown in Fig. 5:

$$E(z) = G(z)X(z) + W(z)\rho(z)H(z)X(z) \tag{41}$$

Subtracting Eqs. (41) from (40), the difference between the two error signal can be obtained:

$$\begin{aligned}\triangle E(z) &= E^*(z) - E(z) \\ &= W(z)H(z)X(z) - W(z)\rho(z)H(z)X(z)\end{aligned} \tag{42}$$

Fig. 5 shows that

$$W(z)\rho(z)X(z) = Y(z) \tag{43}$$

and

$$W(z)X(z) = V(z) \tag{44}$$

Therefore Eq. (42) is simplified to

$$\triangle E(z) = H(z)\{V(z) - Y(z)\} \tag{45}$$

$\triangle E(z)$ can be expressed in the time-domain as

$$\triangle e(n) = h(n) \circledast \{v(n) - y(n)\} \tag{46}$$

Note that both $v(n)$ and $y(n)$ are available in the digital electronic domain, as shown in Figure 5. The secondary path impulse response is also available for the adaptive ANC system as it has to be used in the original FxLMS update equation given in Eq. (12). Therefore, $\triangle e(n)$ can be expressed by

$$\triangle e(n) = \sum_{q=0}^{Q-1} h_q \{v(n-q) - y(n-q)\} \tag{47}$$

$\triangle e(n)$ is the difference between the available error signal in the remote ANC system and the desired error signal. This difference should be added to the available error signal before being used by an FxLMS-like update equation. In this case, the new update equation can be expressed by

$$\mathbf{w}(n+1) = \mathbf{w}(n) + \mu\{e(n) + \triangle e(n)\}\mathbf{x}_G(n) \tag{48}$$

This update equation can adaptively identify an estimate of $\tilde{W}_{opt}(z)$.

IV. Simulation Results

This section discusses the numerical results obtained from a set of computer simulation experiments in order to verify the theoretical results. In the following simulation experiments, a noise source generates an stochastic noise with the normalized bandwidth of 0.4. In this case, the reference signal $x\left(n\right)$ can be initially produced as a random number with the mean of zero and variance of 1. It is then filtered by a low pass filter with a normalized cutoff frequency of 0.4. In the simulation experiments, the noise source is located at the Cartesian coordinates $\left(0,2\right)$, the control source is located at the Cartesian coordinates $\left(-0.4,-0.5\right)$ and the error microphone is located at the origin of the coordinate system. In this situation, the geometrical parameters of the system can be computed as $\mathrm{L_x}$=2 m, $\mathrm{L_y}$=0.64 m and φ_{y}=231 degrees. It is assumed that $u_1\left(n\right)$ and $u_2\left(n\right)$ are two low pass filters.

In the first simulation experiment, the traditional ANC system is considered; therefore, it is desired to create a silent point at the location of the error microphone. By substituting the values of $x\left(n\right)$ in Eq. (1), the noise field can be calculated. By using the values of the parameters $\mathrm{L_x}$, $\mathrm{L_y}$ and φ_{y}, the optimal transfer function $W_{opt}\left(z\right)$, given in Eq. (11), can be constructed. The control signal $y\left(n\right)$ can be then calculated as the response of $W_{opt}\left(z\right)$ to $x\left(n\right)$. By substituting the values of $y\left(n\right)$ in Eq. (2), the anti-noise field (or control field) can be calculated. The summation of the noise field and anti-noise field results in the net sound field. The net sound field over the x-axis is calculated and it is then plotted in Fig. 6 by the blue curve. As seen, the noise is attenuated by more than 30 dB at the location of the error microphone, resulting in the creation of a silent point at this location.

In the second simulation experiment, the FxLMS algorithm (as shown in Fig. 2b) is applied to identify $W_{opt}\left(z\right)$. When the FxLMS algorithm reaches steady state conditions, the weight vector $\mathbf{w}\left(n\right)$ is used to construct $W_{opt}\left(z\right)$. The control signal $y\left(n\right)$ can be then re-calculated as the response of $W_{opt}\left(z\right)$ to the reference signal. Repeating the procedure described in the previous experiment, the net sound field over the x-axis can be calculated and plotted. The results is shown in Fig. 6 by the red curve. Comparing the blue and red curves in Fig. 6 shows that the FxLMS algorithm arrives at the optimal controller that can be obtained through the analysis of the ANC plant in the acoustic domain. Also, from this figure, the limited extension of the zone of quiet surrounding the silent point is evident. In this particular example, the zone of quiet diameter is not more than 4 cm. Considering the space occupied by the error microphone, the zone of quiet has no room for any other device or human ear.

Now, the remote ANC system proposed in this paper is simulated. In the third simulation experiment, it is desired to create a silent point at a location 10 cm away from the error microphone: $\mathrm{L_r}$=0.1 m. By using the values of the parameters $\mathrm{L_x}$, $\mathrm{L_y}$,φ_{y} and $\mathrm{L_r}$ the optimal transfer function $\tilde{W}_{opt}\left(z\right)$, given in Eq. (38), can be constructed. Repeating the same procedure described in the first experiment, the net sound field over the real-axis can be plotted, as shown in Fig. 7 by the blue curve. As seen, the sound field is attenuated by more than

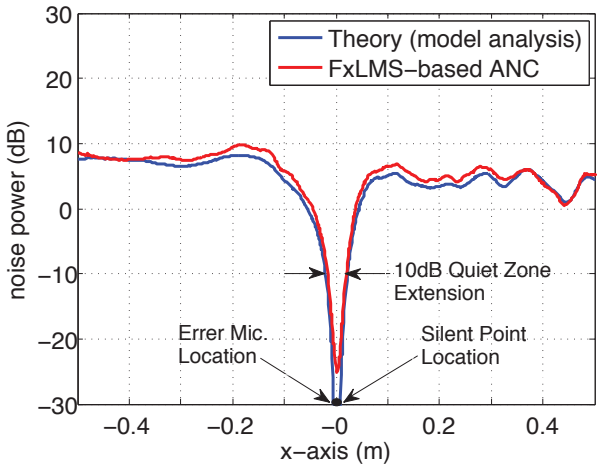

Figure 6: net acoustic pressure (sound field) on the x-axis in traditional ANC: the error microphone has to be located at the silent point

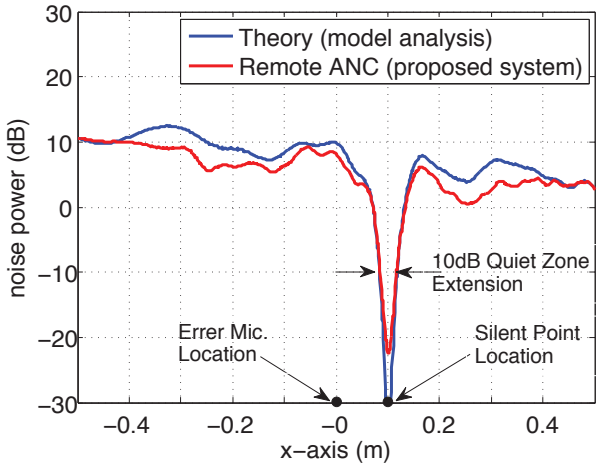

Figure 7: net acoustic pressure (sound field) on the x-axis in remote adaptive ANC (proposed system): the error microphone is located far from the silent point

30 dB at a location 10 cm away from the error microphone, resulting in the creation of a remote silent point.

In the last simulation experiment, the adaptive signal processing system proposed in Subsection III-B is applied to identify $\tilde{W}_{opt}\left(z\right)$. The functional block diagram of the system is shown in Fig. 5. The update equation shown in the block diagram is also given in Eq. (48). When the adaptation process reaches steady state conditions, the last weight vector, updated by Eq. (48), is used to construct $\tilde{W}_{opt}\left(z\right)$. Repeating the procedure described in the previous experiment, the net sound field over the x-axis is calculated and it is then plotted in Fig. 7 by a red curve. Comparing the blue and red curves in Fig. 7 shows that the proposed adaptive signal processing system algorithm arrives at the optimal controller that can be obtained through the analysis of the ANC plant in the acoustic domain. Hence, we can come to this conclusion that the adaptive creation of a remote silent point is possible. Since the error microphone is not located at the remote silent point,

the space available in the surrounding zone of quiet (remote zone of quiet) can be used more efficiently.

V. Conclusion

Single-channel ANC systems are only able to make small zones of quiet around an error microphone. Moreover, the error microphone occupies a part of the available space in the zone of quiet, resulting in a very small effective space within the zone of quiet. In this paper, we developed a new ANC system for making a remote silent point located far from the error microphone. The proposed ANC controller is a series combination of a remote controller and an original FxLMS-based ANC controller. The remote controller has a pure-delay impulse response with a positive semi-definite time-delay. The static gain and time-delay of the remote controller were found by analyzing the ANC plant in the acoustic domain. The second part of the remote ANC system is an original FxLMS-based controller, but we could not apply the original FxLMS algorithm in the remote ANC system. This is because the error signal is affected by the remote controller in the remote ANC system. A mechanism for the compensation for the effects of the remote controller on the error signal was proposed, resulting in an new adaptive algorithm for remote ANC applications.

VI. Acknowledgment

This research is supported by The University of Auckland FRDF grant; Project Number: 3700501.

References

[1] S. M. Kuo and D. R. Morgan, *Active noise control systems: algorithms and DSP implementations*. New York, NY, USA: Wiley Interscience, 1996.

[2] H. F. Olson, "Electronic control of noise, vibration and reverberation," *Journal of the Acoustical Society of America*, vol. 28, pp. 966–972, 1956.

[3] S. Elliott and T. Sutton, "Performance of feedforward and feedback systems for active control," *Speech and Audio Processing, IEEE Transactions on*, vol. 4, no. 3, pp. 214–223, 1996.

[4] J. C. Burgess, "Active adaptive sound control in a duct: computer simulation," *Journal of the Acoustical Society of America*, vol. 70, pp. 715–726, 1981.

[5] G. E. Warnaka, L. A. Poole, and J. Tichy, "Active acoustic attenuators," *U.S. Patent 4473906*, 1984.

[6] B. Widrow, J. Glover, J. McCool, J. Kaunitz, C. Williams, R. Hearn, J. Zeidler, J. Eugene Dong, and R. Goodlin, "Adaptive noise cancelling: principles and applications," *Proceedings of the IEEE*, vol. 63, no. 12, pp. 1692–1716, Dec. 1975.

[7] S. Elliott, I. M. Stothers, and P. A. Neslson, "A multiple error LMS algorithm and its applications to active control of sound and vibration," *IEEE Transactions on Acoustic, Speech and Signal Processing Processing*, vol. 35, pp. 1423–1434, 1987.

[8] L. J. Eriksson, "Recursive algorithms for active noise control," *International Symposium of Active Control of Sound and Vibration*, pp. 137–146, 1991.

[9] B. Widrow, D. Shur, and S. Shaffer, "On adaptive inverse control," in *Proceeding of the 15th Asilomar Conference on Circuits, Systems and Computers*, Nov. 1981, pp. 185–189.

[10] I. Tabatabaei Ardekani and W. H. Abdulla, "Theoretical convergence analysis of FxLMS algorithm," *Signal Processing*, vol. 90, no. 12, pp. 3046 – 3055, 2010.

[11] ——, "On the convergence of real-time active noise control systems," *Signal Processing*, vol. 91, no. 5, pp. 1262–1274, 2011.

[12] ——, "On the stability of adaptation process in active noise control systems," *Journal of Acoustical Society of America*, vol. 129, no. 1, pp. 173–184, 2011.

[13] ——, "Effects of imperfect secondary path modeling on adaptive active noise control systems," *IEEE Transactions on Control Systems Technology*, vol. 20, no. 5, pp. 1252 –1262, sept. 2012.

[14] ——, "Root locus analysis and design of the adaptation process in active noise control," *Journal of Acoustical Society of America*, vol. 132, no. 4, 2012.

[15] P. Joseph, S. Elliott, and P. Nelson, "Statistical aspects of active control in harmonic enclosed sound fields," *Journal of Sound and Vibration*, vol. 172, no. 5, pp. 629 – 655, 1994.

[16] S. Elliott, C. Boucher, and P. Nelson, "The behavior of a multiple channel active control system," *Signal Processing, IEEE Transactions on*, vol. 40, no. 5, pp. 1041–1052, 1992.

[17] J. Garcia Bonito, S. J. Elliott, and C. C. Boucher, "Generation of zones of quiet using a virtual microphone arrangement," *The Journal of the Acoustical Society of America*, vol. 101, no. 6, pp. 3498–3516, 1997.

[18] J. Diaz, J. Egana, and J. Vinolas, "A local active noise control systems based on a virtual-microphone technique for railway sleeping vehicle applications," *Mechanical Systems and Signal Processing*, vol. 20, pp. 2259–2276, 2006.

[19] D. Das, D. Mpreau, and B. Cazzolato, "Adjoint nonlinear active noise control algorithm for virtual microphone," *Mechanical Systems and Signal Processing*, vol. 2012, pp. 743–754, 27.

[20] R. Serizel, M. Moonen, J. Wouters, and S. Jensen, "A zone-of-quiet based approach to integrated active noise control and noise reduction for speech enhancement in hearing aids," *Audio, Speech, and Language Processing, IEEE Transactions on*, vol. 20, no. 6, pp. 1685–1697, 2012.

[21] ——, "Integrated active noise control and noise reduction in hearing aids," *Audio, Speech, and Language Processing, IEEE Transactions on*, vol. 18, no. 6, pp. 1137–1146, 2010.